Guide for the identification of archaeological sea sturgeon (*Acipenser sturio* and *A. oxyrinchus*) remains

by

Els THIEREN (1, 2), Wim WOUTERS (1) & Wim VAN NEER* (1, 2)

Abstract. - Remains of sturgeons (*Acipenser sturio* and *A. oxyrinchus*) are regularly found on western European archaeological sites. The identification of these isolated bones should ideally be carried out with the aid of a comparative skeletal collection, consisting of modern specimens of different sizes. Because such reference material of sea sturgeons (*A. sturio* and *A. oxyrinchus*) is relatively rare and dispersed over many different museums and institutes, a practical guide is presented here as an aid to the identification of the most commonly found archaeological sturgeon remains. This guide, which is based on observations made on 64 individuals housed in 13 different natural history collections, should allow identifying most archaeological sturgeon remains from western European sites. Presented are the morphological characteristics of the bones of the skull roof and circumorbital region (posttemporal, dermopterotic, parietal, frontal, dermosphenotic, postorbital, jugal and supraorbital), bones of the braincase (parasphenoid), opercular series (subopercle and branchiostegals), the palatoquadrate and associated bones and lower jaw (palatopterygoid, dermopalatine and dentary), the hyoid and gill arches with the hyomandibula, the isolated skeletal elements from the pectoral girdle (clavicle, cleithrum and supracleithrum), the bones of the fin and fin supports (pectoral fin spine, fin rays and fulcra) and the dorsal, ventral, lateral and accessory scutes. For each element, descriptions and pictures are provided of modern and archaeological specimens. Regression equations allowing fish length reconstructions on the basis of single bone measurements are given for 14 elements and the scutes. Finally, criteria for species identification are provided. In the case of the dentary, dermopalatine and palatopterygoid, these are differences in shape of the skeletal elements, whereas for the dermal bones the external surface pattern is diagnostic when reconstructed fish length is over one meter.

Résumé. - Guide pour l'identification de restes archéologiques d'esturgeons (*Acipenser sturio* et *A. oxyrinchus*).

Les ossements d'esturgeons (*Acipenser sturio* et *A. oxyrinchus*) sont régulièrement retrouvés sur des sites archéologiques en Europe occidentale. L'identification de ces os isolés se fait idéalement à l'aide d'une collection de référence comprenant des squelettes de poissons de tailles différentes. Ce matériel de référence d'*A. sturio* et *A. oxyrinchus* étant relativement rare et dispersé au sein de nombreux musées et institutions différents, un guide pratique est présenté ici pour aider à l'identification des restes d'esturgeons les plus couramment trouvés en contexte archéologique. Ce guide, basé sur des observations faites sur 64 individus dans 13 collections d'histoire naturelle, devrait permettre d'identifier la majeure partie des restes d'esturgeons récoltés sur des sites archéologiques en Europe occidentale. Les caractères morphologiques sont décrits pour les éléments squelettiques isolés de la ceinture scapulaire (clavicule, cleithrum et supracleithrum), les ossements du toit crânien et de la région circum-orbitaire (post-temporal, dermoptérotique, pariétal, frontal, dermosphénotique, post-orbitaire, jugal et supra-orbitaire), les ossements de la série operculaire (sous-opercule et rayons branchiostèges), le neurocrâne (parasphénoïde), le palato-carré et ossements associés (palatoptérygoïde, dermopalatin et dentaire), les arcs branchiaux et hyoïdal (hyomandibulaire), les ossements des nageoires et de leurs supports (épine pectorale, rayons des nageoires et les fulcra) et finalement pour les écussons osseux dorsaux, ventraux, latéraux et accessoires. Pour chaque élément, des descriptions et des photos de spécimens modernes et archéologiques sont fournies. Des équations prédictrices de reconstitution des tailles, d'après les mesures des os isolés, sont données pour 14 éléments et pour les écussons. Finalement, les critères permettant une identification spécifique sont décrits. Dans le cas des palatoptérygoïde, dermopalatin et dentaire, il s'agit de différences dans la forme des éléments squelettiques. Pour les os dermiques du crâne, de la ceinture scapulaire et les écussons des rangées longitudinales, l'ornementation externe est diagnostique à condition que la longueur reconstituée des poissons soit supérieure à un mètre.

Faunal remains found on archaeological sites allow reconstructing human subsistence strategies but can also contribute to biodiversity and nature conservation issues (Lyman, 2006). Archaeozoological remains have the potential of documenting invasions and extinctions in a particular region and can provide evidence at the centennial or millennial scale, which largely exceeds the historical information fishery biologists have, at best, at their disposal. An example, in Western Europe and the Baltic region, where the fate of a fish taxon can be followed through time is the sturgeon. Indeed, research published since 2002 has shown that besides the 'traditional' *Acipenser sturio* Linnaeus, 1758, *Acipenser*

(1) Royal Belgian Institute of Natural Sciences, Vautierstraat 29, B-1000 Brussels, Belgium. [els.thieren@naturalsciences.be] [wim.wouters@naturalsciences.be]

(2) Laboratory of Biodiversity and Evolutionary Genomics, KU Leuven, Ch. Debériotstraat 32, B-3000 Leuven, Belgium.

* Corresponding author [wim.vanneer@naturalsciences.be]

oxyrinchus Mitchill, 1815 has also occurred in the region for several millennia and not only in the Baltic Sea (Ludwig *et al.*, 2002, 2008, 2009; Tiedemann *et al.*, 2007; Popović *et al.*, 2014), but also along the French Atlantic façade (Desse-Berset, 2009, 2011a; Chassaing *et al.*, 2013).

The information obtained on the species occurrences was based on sturgeon specimens housed in museums and on archaeological bone finds, on which both traditional morphological and (palaeo-) genetic analyses were carried out. In general, archaeological sturgeon remains are relatively easy to recognise, mainly because of their sturdiness and large size, and the distinctive surface pattern of the dermal bones. In most cases, the remains are large enough to be retrieved by hand on archaeological excavations and therefore, sturgeon (*A. sturio*/*A. oxyrinchus*) bones are regularly found on archaeological sites in western Europe and the Baltic region (e.g. Clason, 1967; Benecke, 1986; Desse-Berset, 1994; Ervynck *et al.*, 1994; Makowiecki, 2008). As with all archaeological animal remains, a correct identification relies to a large extent on adequate reference collections, preferably consisting of modern skeletons of animals of different size and sex. However, access to comparative skeletons of certain species, especially those which are rare or almost extinct, such as sturgeons, is not always easy or possible. Moreover, because of increasing privatization of the archaeological sector, archaeozoological analysis is in many cases outsourced to self-employed people or small private companies, for whom it is often difficult to establish and maintain a large reference collection.

To allow identification of isolated sturgeon remains in the absence of a reference collection, an identification guide can be useful. Although several publications exist on the osteology of sturgeon (e.g. Findeis, 1997; Hilton *et al.*, 2011), these are mainly focused on details of skeletal anatomy and are therefore not always suitable for the identification of archaeological bones. Some published (e.g. Desse-Berset, 2011b) or online (e.g. Archaeological Fish Resource, 2011) material is available, but these only cover the sturgeon skeleton partly, and some of the skeletal elements regularly found on excavations are not included. In the present contribution we want to provide a practical guide for the identification and size reconstruction of sturgeons (*A. sturio*/*A. oxyrinchus*) based on the elements most commonly found on archaeological excavations. Although archaeological remains can quite easily be identified as 'sturgeon', identifying the exact skeletal element is not always straightforward. However, this is crucial to establish the minimum number of individuals and to estimate fish length, which, in turn, is needed for species identification. This work partly summarizes results presented in Thieren and Van Neer (2014, in press), and Thieren *et al.* (unpubl. data).

MATERIAL AND METHODS

In the following section, an overview is given of the sturgeon skeletal elements most commonly found on archaeological sites. The nomenclature according to Hilton *et al.* (2011) is used. For each element, descriptions and pictures are provided of modern and – in most cases – archaeological specimens, which should be sufficient to identify archaeological remains. However, because sturgeons display a high intraspecific variation in the shape of their bones, some of the listed criteria are not always clearly visible on all bones. The pictures provided here are from a modern museum specimen of *A. oxyrinchus* (RBINS 24792) with a total length (TL) of 74 cm. This is the largest disarticulated specimen available in the collections of the Royal Belgian Institute of Natural Sciences. To our knowledge, no larger disarticulated individuals are available in the museums that we visited elsewhere in Europe (see list in the acknowledgements). As this modern individual is relatively small, diagnostic features typical of larger specimens are not always clearly visible. Therefore, pictures of archaeological remains from larger specimens are also provided in most cases.
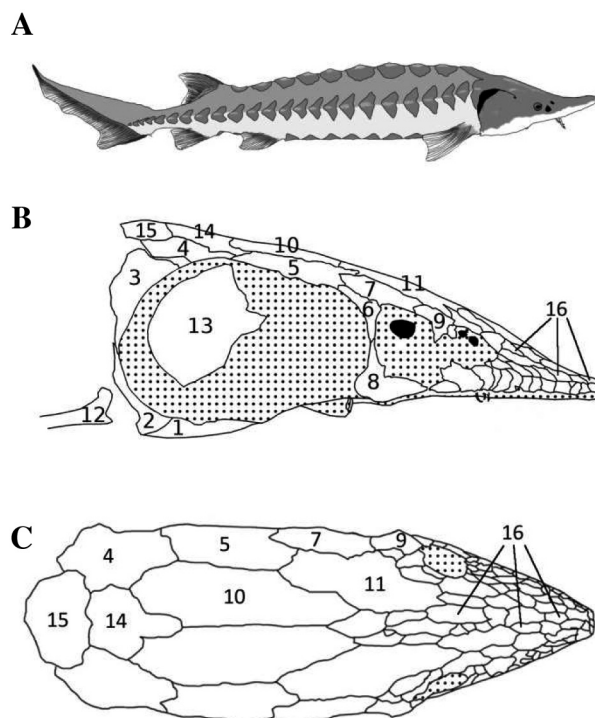

Figure 1. - **A**: Complete specimen; **B**: Schematic overview of the bones of the head and pectoral girdle, lateral view; **C**: Dorsal view. 1: clavicle; 2: cleithrum; 3: supracleithrum; 4: posttemporal; 5: dermopterotic; 6: postorbital; 7: dermosphenotic; 8: jugal; 9: supraorbital; 10: parietal; 11: frontal; 12: pectoral fin spine; 13: subopercle; 14: median extrascapular; 15: first dorsal scute; 16: dorsal rostral bones. Dotted areas are not ossified.
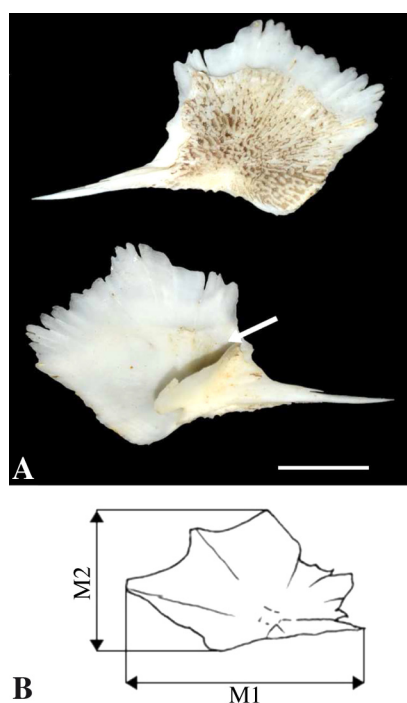
Figure 2. - Posttemporal. **A**: Dorsal and ventral view of the left posttemporal from *A. oxyrinchus* (RBINS 24792). Arrow: ventral lamella; **B**: Possible measurements on the posttemporal for size reconstruction. Scale bar = 1 cm.
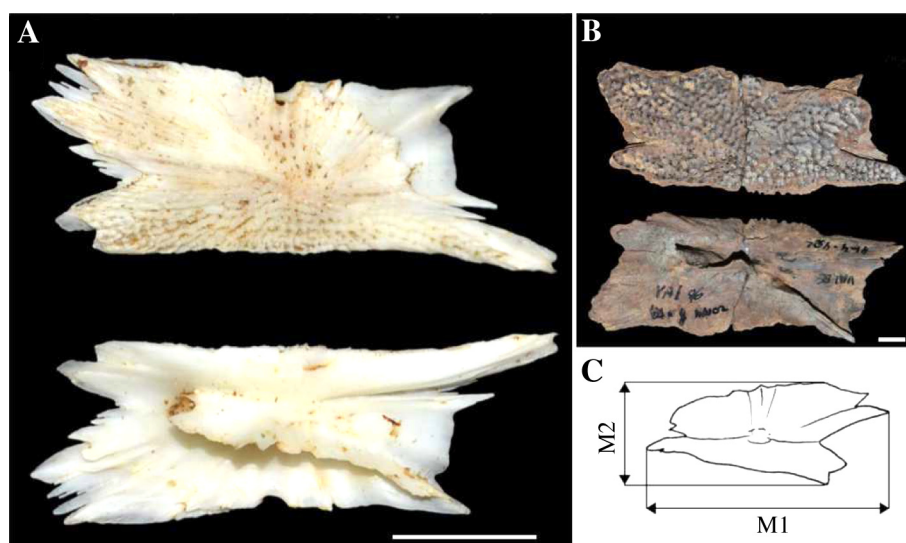

Figure 3. - Dermopterotic. **A**: Dorsal and ventral view of the left dermopterotic from *A. oxyrinchus* (RBINS 24792); **B**: Dorsal and ventral view of a left archaeological dermopterotic; **C**: Possible measurements on the dermopterotic for size reconstruction. Scale bars = 1 cm.
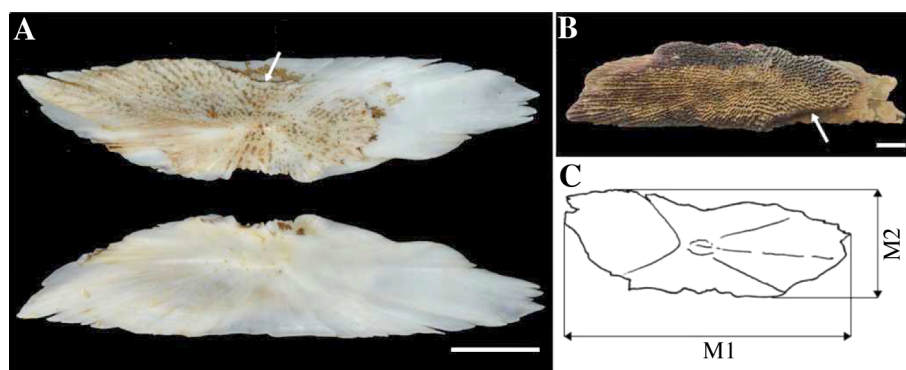

Figure 4. - Parietal. **A**: Dorsal and ventral view of the left parietal from *A. oxyrinchus* (RBINS 24792); **B**: Dorsal view of an archaeological right parietal; **C**: Possible measurements on the parietal for size reconstruction. Arrow: notch for the median extrascapular. Scale bars = 1 cm.
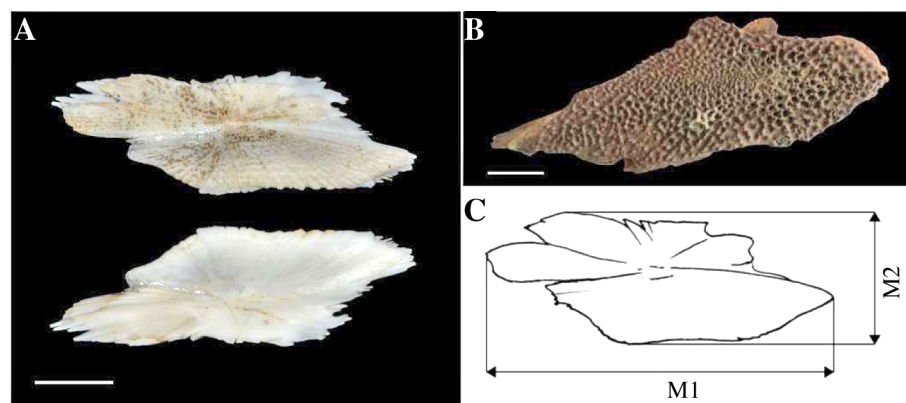

Figure 5. - Frontal. **A**: Dorsal and ventral view of the left frontal from *A. oxyrinchus* (RBINS 24792); **B**: Dorsal view of an archaeological left frontal; **C**: Possible measurements on the frontal for size reconstruction. Scale bars = 1 cm.

Figure 6. - Dermosphenotic. **A**: Dorsal and ventral view of the left dermosphenotic from *A. oxyrinchus* (RBINS 24792); **B**: Dorsal view of an archaeological right dermosphenotic; **C**: Possible measurements on the dermosphenotic for size reconstruction. Arrows: curved lateral edge. Scale bars = 1 cm.
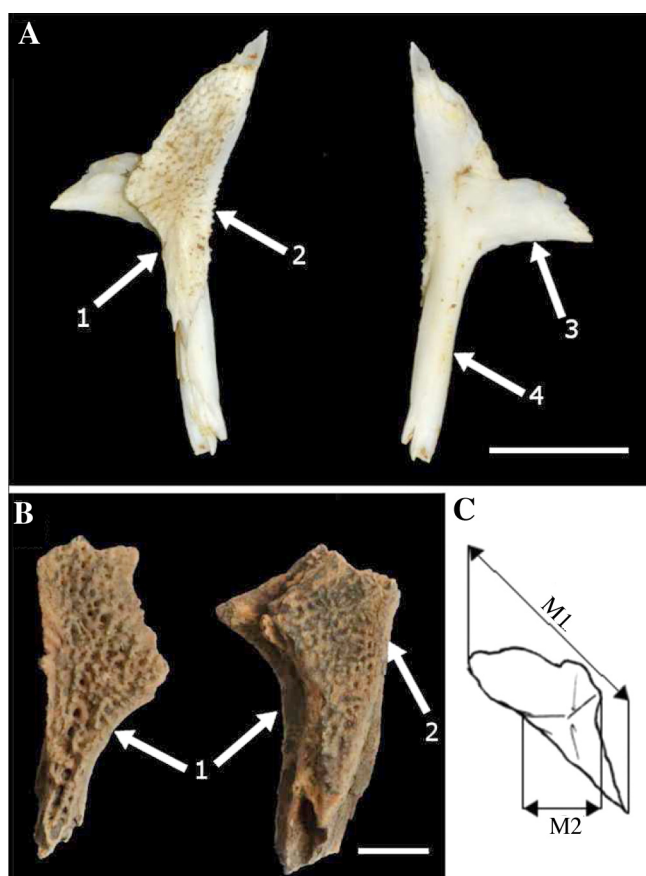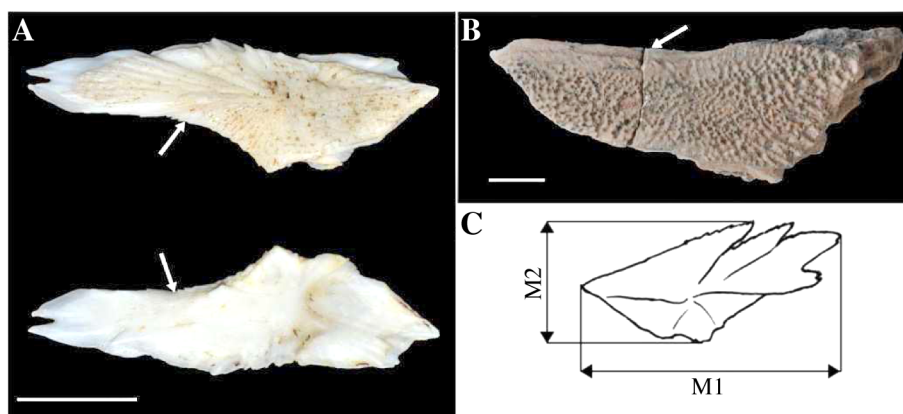

Figure 7. - Postorbital. **A**: Lateral and medial view of the left postorbital from *A. oxyrinchus* (RBINS 24792); **B**: Lateral view of fragments of a right and left archaeological postorbital; **C**: Possible measurements on the postorbital for size reconstruction. Arrow 1: concave anterior margin; arrow 2: concave posterior margin; arrow 3: anterior medial processus; arrow 4: ventral medial processus. Scale bars = 1 cm.
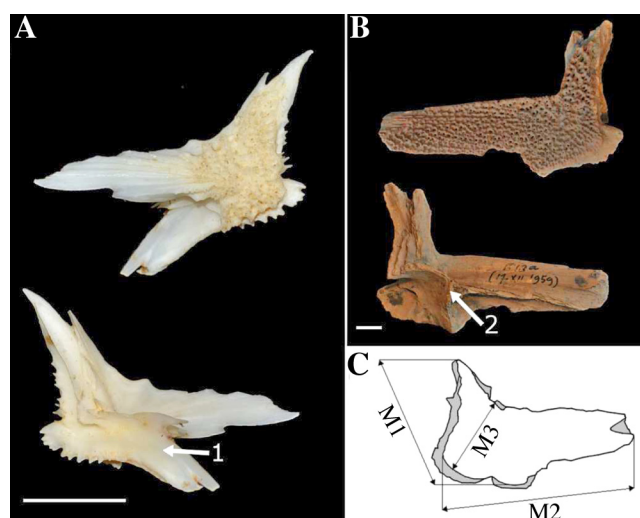

Figure 8. - Jugal. **A**: Lateral and medial view of the left jugal from *A. oxyrinchus* (RBINS 24792); **B**: Lateral and medial view of archaeological left jugal; **C**: Possible measurements on the jugal for size reconstruction. Arrow 1: medial lamella; arrow 2: broken medial lamella. Scale bars = 1 cm.

For each skeletal element on which measurements can be taken, the defined measuring distances are depicted and the regression equations are provided that allow the back-calculation of the total length of the fish. These equations, taken from Thieren and Van Neer (2014) for bones of the skull and

the pectoral girdle, and from Thieren and Van Neer (in press) for the scutes, are based on both *A. oxyrinchus* and *A. sturio* reference specimens and therefore valid for both species. For the bones of the skull, statistical tests on genetically identified museum specimens did not indicate species-specific differences in the equations (Thieren and Van Neer, 2014). By combining data from both species, the number of individuals was larger and the accuracy of the model increased. For the scutes, species-specific differences were noticed. However, since the back-calculated size from archaeological remains has to be known prior to species identification (see below), species-specific regression models would be of no use to back-calculate lengths from remains not identified to species (Thieren *et al*., unpubl. data).

In our overview below, we also include the information mentioned in earlier studies by Desse-Berset (1994, 2011b). This author took some measurements on three splanchnocranial bones (dentary, dermopalatine and palatopterygoid) of
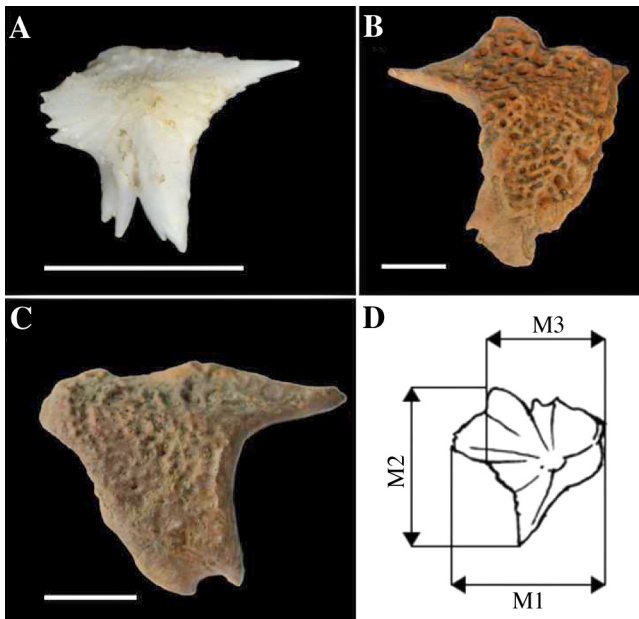
Figure 9. - Supraorbital. **A**: Lateral view of the left supraorbital from *A. oxyrinchus* (RBINS 24792); **B**: Archaeological right and **C**: Left supraorbital, lateral view; **D**: Possible measurements on the supraorbital for size reconstruction. Scale bars = 1 cm.
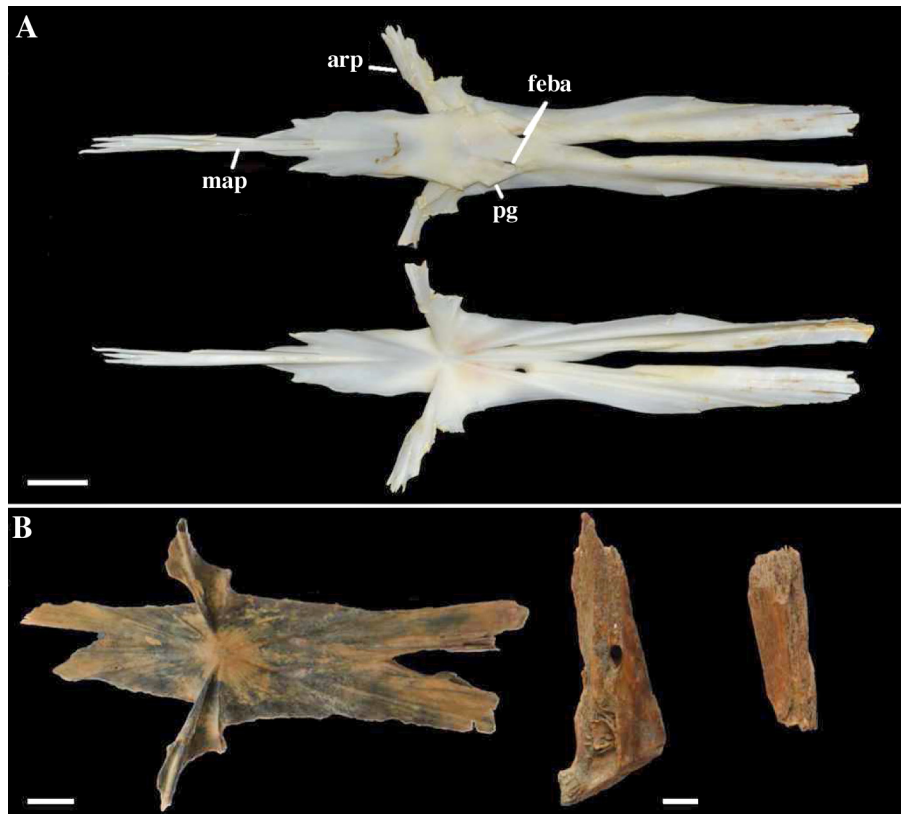

Figure 10. - Parasphenoid. **A**: Ventral and dorsal view of the parasphenoid from *A. oxyrinchus* (RBINS 24792). Abbreviations: map: median anterior processus; arp: lateral ascending rami; feba: foramina for the branchial arteries; pg: articulation points for the branchial arches; **B**: Archaeological parasphenoid, almost complete (dorsal view) and fragments. Scale bars = 1 cm.

modern *A. sturio* and *A. oxyrinchus* of known length; she provided the resulting data in graphical form and gave some regression equations. Because there is a lack of sufficient disarticulated reference specimens, no equations can be provided for size reconstruction based on bones of the endoskeleton, such as the parasphenoid, hyoid and hyomandibula.

Finally, criteria are provided for the identification to species. The differences in shape, described by Desse-Berset (2011b) for the dentary, dermopalatine and palatopterygoid, are summarized. For the other bones, the external ornamentation is used, a criterion initially mentioned by Magnin (1964). In the present contribution, we use the criteria developed by Thieren *et al.* (unpublished) that also take into account the ontogenetic changes in surface morphology.

RESULTS AND DISCUSSION

Figure 1 gives an overview of a complete sturgeon specimen (Fig. 1A) and the placement of the different dermal bones of the skull in a lateral (Fig. 1B) and dorsal (Fig. 1C) view. The individual skeletal elements are presented and discussed below in the following order: bones of the skull roof and circumorbital region, bones of the braincase, the opercular series, the palatoquadrate and associated bones, the hyoid and gill arches, the bones of the pectoral girdle, fins and fin supports, and finally the scutes. After this follows a discussion of how to use the external ornamentation pattern for species identification.

Bones of the skull roof and circumorbital region
Posttemporal

The posttemporal (Fig. 2) is a flat, ornamented, squarish bone with a frontal spine and a ventral lamella (Fig. 2A), similar to that of the dermopterotic. The posttemporal is often fragmented in archaeological assemblages, which makes it difficult to distinguish the element from the dermopterotic.

Size can be back-calculated with equations 1 to 3 with measurements taken on the posttemporal as indicated on figure 2B.

Equation 1: $TL = 4.6407\, M1^{0.7902}$ $(R^2 = 0.94, n = 43)$

Equation 2: $TL = 3.5846 \, M2^{1.0105}$
($R^2 = 0.93$, n = 44)

Equation 3: $TL = 3.7810 \, M1^{0.4288}$
$M2^{0.4883}$ ($R^2 = 0.96$, n = 43)

Dermopterotic

The dermopterotic (Fig. 3) is flat on the ornamented dorsal side and has a distinctive lamella on the ventral side of the bone. It runs from the centre of the bone to the posterior-lateral point of the bone and is often broken in archaeological remains (Fig. 3B).

Size can be back-calculated using equations 4 to 6 with measurements taken on the dermopterotic as indicated on figure 3C.

Equation 4: $TL = 2.2744 \, M1^{0.9580}$
($R^2 = 0.92$, n = 45)

Equation 5: $TL = 5.5551 \, M2^{0.9522}$
($R^2 = 0.92$, n = 45)

Equation 6: $TL = 3.2705 \, M1^{0.4900} \, M2^{0.4893}$ ($R^2 = 0.94$, n = 45)

Parietal and frontal

Parietals (Fig. 4) and frontals (Fig. 5) are not always easy to distinguish from each other. Both bones are ornamented, oblong and flat. The medial side of the parietal is usually straight, with a small notch for the median extrascapular. The frontal usually has a slightly different, more trapezium-to triangular-like shape.

For the parietal, size can be back-calculated with equations 7 to 9 with measurements taken on the parietal as indicated on figure 4C. For the frontal, size can be back-calculated with equations 10 to 12 with measurements taken on the frontal as indicated on figure 5C. When the bone cannot be identified as either parietal or frontal, the size can be back-calculated with equations 13 to 15, using the same measurements as in figure 4C or figure 5C.

Equation 7: $TL = 1.8339 \, M1^{0.9284}$ ($R^2 = 0.94$, n = 48)

Equation 8: $TL = 5.2404 \, M2^{0.9606}$ ($R^2 = 0.96$, n = 47)

Equation 9: $TL = 3.4484 \, M1^{0.3256} \, M2^{0.6399}$ ($R^2 = 0.97$, n = 47)

Equation 10: $TL = 1.6914 \, M1^{0.9509}$ ($R^2 = 0.92$, n = 50)

Equation 11: $TL = 5.1121 \, M2^{0.9530}$ ($R^2 = 0.95$, n = 49)

Equation 12: $TL = 2.8511 \, M1^{0.4232} \, M2^{0.5592}$ ($R^2 = 0.96$, n = 49)

Equation 13: $TL = 1.7626 \, M1^{0.9395}$ ($R^2 = 0.93$, n = 49)

Equation 14: $TL = 5.2109 \, M2^{0.9544}$ ($R^2 = 0.95$, n = 48)

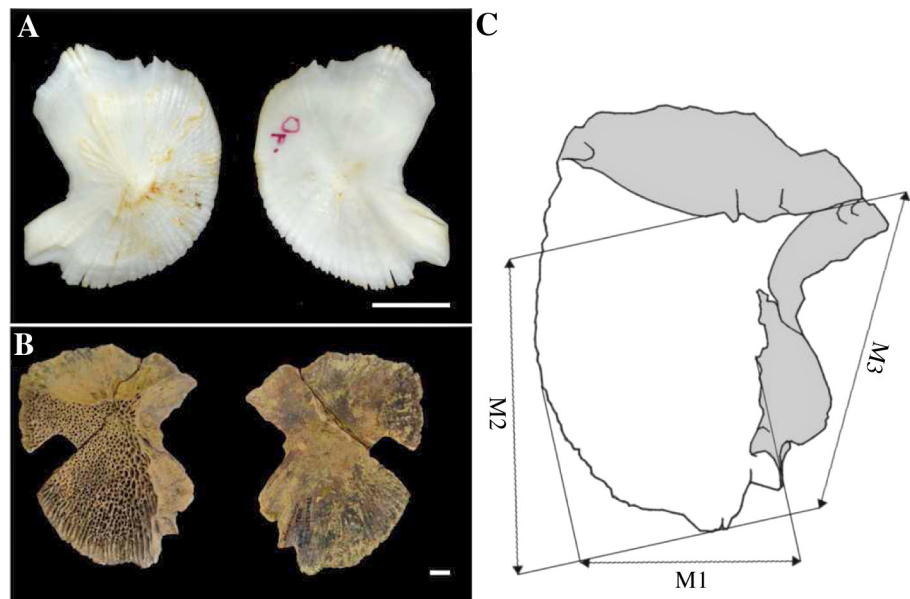Equation 15: $TL = 3.0986 \, M1^{0.3870} \, M2^{0.5854}$ ($R^2 = 0.97$, n = 48)

Figure 11. - Subopercle. **A**: Lateral and medial view of the left subopercle from *A. oxyrinchus* (RBINS 24792); **B**: Lateral and medial view of an archaeological right subopercle; **C**: Possible measurements on the subopercle for size reconstruction. Scale bars = 1 cm.
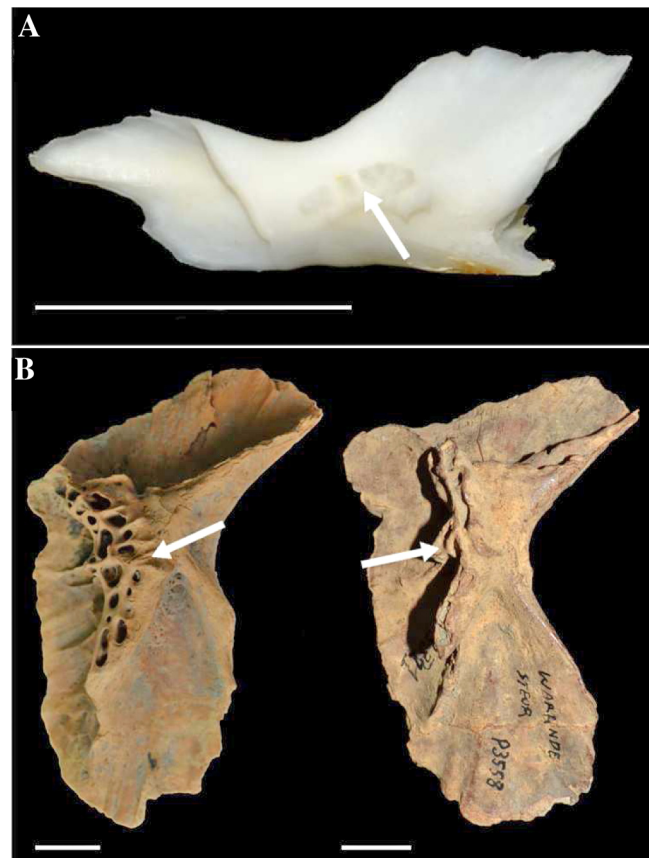

Figure 12. - Branchiostegals, lateral view. **A**: Branchiostegal from *A. oxyrinchus* (RBINS 24792); **B**: Two archaeological branchiostegals. Arrows: protruding ornamented area. Scale bars = 1 cm.
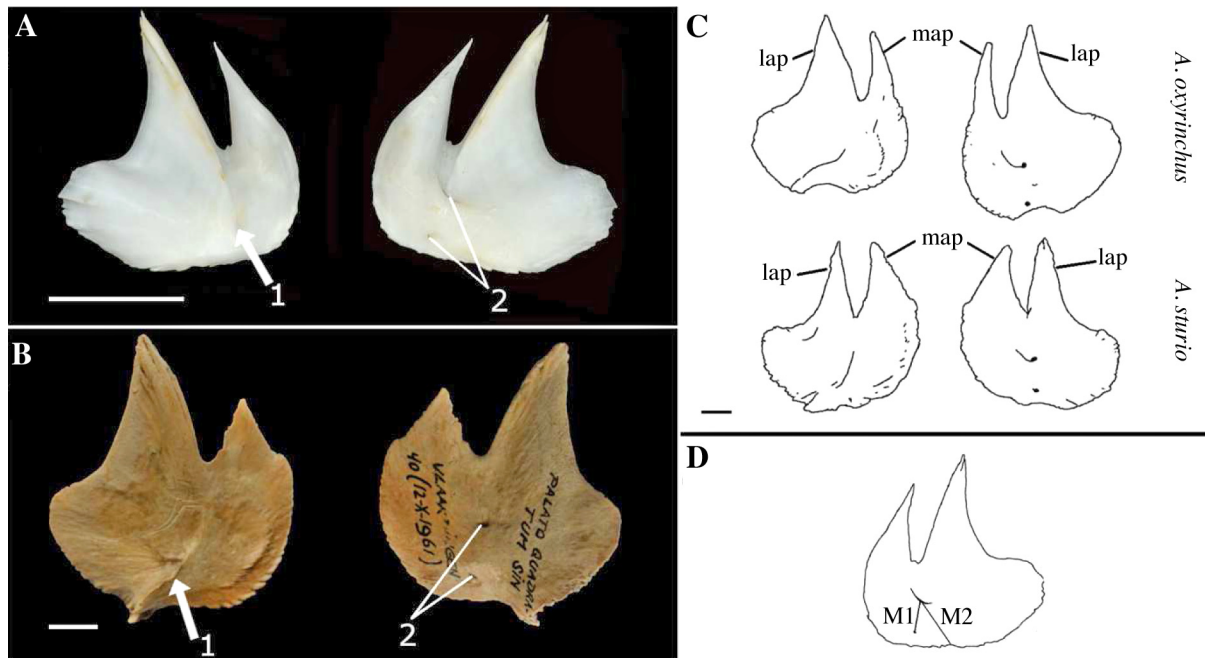
Figure 13. - Palatopterygoid. **A**: Dorsal and ventral view of the left palatopterygoid from *A. oxyrinchus* (RBINS 24792); **B**: Dorsal and ventral view of an archaeological left palatopterygoid identified as *Acipenser* sp.; **C**: Dorsal and ventral view of the left palatopterygoid of *A. oxyrinchus* and *A. sturio*, redrawn from Desse-Berset (2011b), abbreviations: map: medial processus, lap: lateral processus; **D**: Measurements on the palatopterygoid as defined by Desse-Berset (2011b). Arrow 1: dorsal bony ridge; arrow 2: ventral foramina. Scale bars = 1 cm.
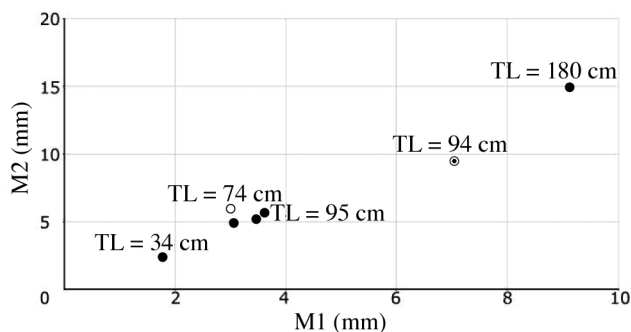

Figure 14. - Relationship between measurements M1 and M2 on palatopterygoid from modern sturgeons of known length (adapted from Desse-Berset, 1994). ● Data for modern *A. sturio* from Desse-Berset, 1994; ○ RBINS 24792, *A. oxyrinchus*; ◉ BAI 1884, morphologically identified *A. sturio*.

Dermosphenotic

The dermosphenotic (Fig. 6) is similar to the frontal and parietal: an oblong, flat and ornamented bone, but with a slightly curved and smooth lateral edge that forms the upper margin of the orbit.

Size can be back-calculated with equations 16 to 18 and measurements taken on the dermosphenotic as indicated on figure 6C.

Equation 16: $TL = 2.6351 \, M1^{0.9722}$ ($R^2 = 0.96$, n = 36)

Equation 17: $TL = 7.6625 \, M2^{0.9432}$ ($R^2 = 0.92$, n = 36)

Equation 18: $TL = 3.4803 \, M1^{0.6554} \, M2^{0.3336}$ ($R^2 = 0.97$, n = 36)

Postorbital

The postorbital is a thin, elongated bone with a small, smooth, concave anterior margin bordering the orbit (Fig. 7A, B). It also has a smooth, concave posterior margin, which lines the operculum. The bone has an unornamented anterior and ventral medial processus (Fig. 7A). Archaeological postorbitals are often broken, mostly leaving only the ventral part of the bone recognisable (Fig. 7B).

Size can be back-calculated with equations 19 and 20 with measurements taken on the postorbital as indicated on figure 7C.

Equation 19: $TL = 3.0280 \, M1^{1.0201}$ ($R^2 = 0.97$, n = 36)

Equation 20: $TL = 8.2121 \, M2^{1.0885}$ ($R^2 = 0.89$, n = 37)

Jugal

The jugal (Fig. 8) is an L-shaped bone, with the shortest arm directed dorsally and the longest arm directed horizontally and anteriorly. The medial lamella on the back of the bone (Fig. 8A) is often broken in archaeological specimens (Fig. 8B).

Size can be back-calculated with equations 21 to 24, using measurements taken on the jugal as shown on figure 8C.

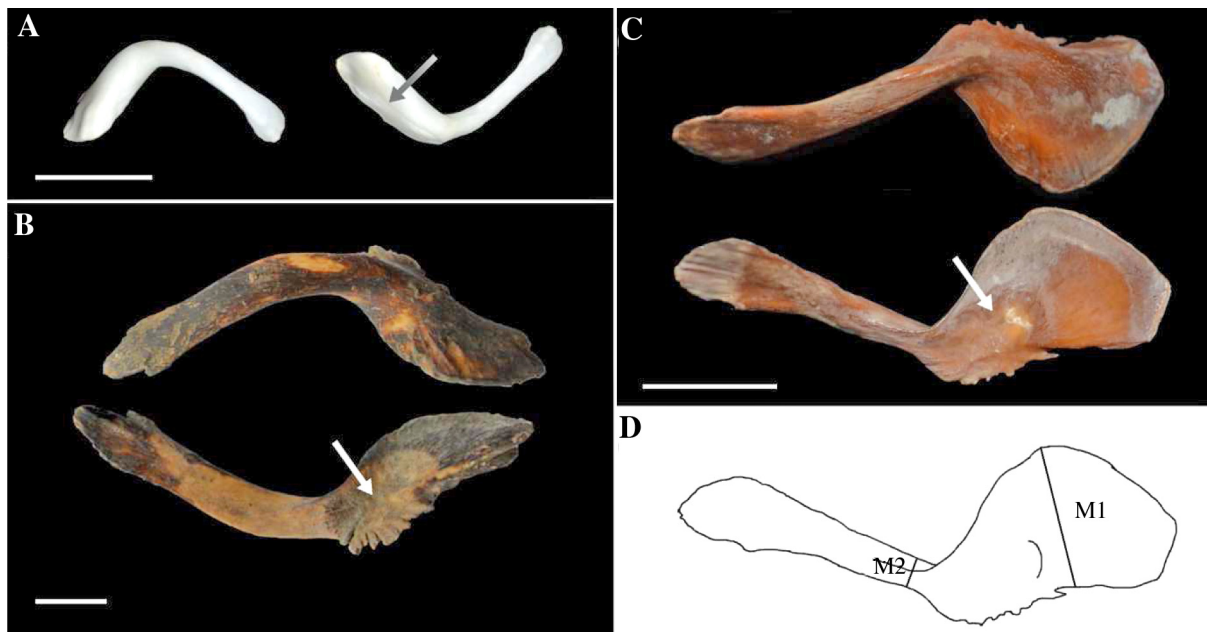Equation 21: $TL = 2.1219 \, M1^{1.1955}$ ($R^2 = 0.94$, n = 50)

Figure 15. - Dermopalatine. **A**: Dorsal and ventral view of left dermopalatine from *A. oxyrinchus* (RBINS 24792); **B**: Dorsal and ventral view of an archaeological right dermopalatine from *A. oxyrinchus*; **C**: Dorsal and ventral view of an archaeological right dermopalatine from *A. sturio*; **D**: Measurements on the dermopalatine as defined by Desse-Berset (2011b). Arrows: fossa. Scale bars = 1 cm.
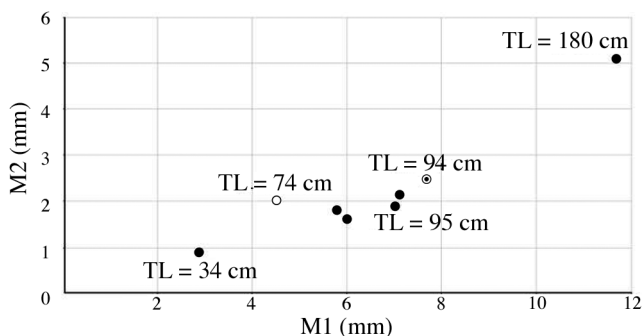

Figure 16. - Relationship between measurements M1 and M2 on dermopalatines from modern sturgeons of known length (adapted from Desse-Berset, 1994). ● Data of modern *A. sturio* from Desse-Berset, 1994; ○ RBINS 24792, *A. oxyrinchus*; ◉ BAI 1884, morphologically identified *A. sturio*.

Equation 22: TL = 1.6779 M2$^{1.0998}$ (R^2 = 0.89, n = 52)
Equation 23: TL = 6.7352 M3$^{1.0054}$ (R^2 = 0.88, n = 50)
Equation 24: TL = 1.6442 M1$^{0.6784}$ M2$^{0.5167}$ (R^2 = 0.96, n = 48)

Supraorbital

The supraorbital (Fig. 9) has a distinctive shape with one posteriorly directed processus and the main body of the bone ventrally directed. The concave posterior edge of the bone forms the anterior border of the orbit. The bone is slightly curved and has a smooth medial side.

Size can be back-calculated with equations 25 to 28 using measurements taken on the supraorbital as indicated on figure 9D.

Equation 25: TL = 5.3179 M1$^{0.9800}$ (R^2 = 0.90, n = 51)
Equation 26: TL = 5.4958 M2$^{1.0700}$ (R^2 = 0.93, n = 49)
Equation 27: TL = 12.4074 M3$^{0.8845}$ (R^2 = 0.93, n = 51)
Equation 28: TL = 5.3879 M1$^{0.3337}$ M2$^{0.5427}$ M3$^{0.1894}$ (R^2 = 0.97, n = 51)

Bones of the braincase
Parasphenoid

The parasphenoid is the only easily recognisable and most commonly found bone of the braincase (Fig. 10). The bone is characterised by two lateral ascending rami (arp), two posterior processes, one median anterior processus (map) and the foramina for the efferent branchial arteries (feba). The bone has grooves marking the articulation point with the branchial arches (pg) on the rami and grooves on the processes, which makes archaeological fragments easily recognisable (Fig. 10B).

Opercular series
Subopercle

The subopercle (Fig. 11) is a more or less circular shaped and slightly concave (in small individuals) to flat (in large individuals) bone. The ornamented part of the bone is roughly shaped as a quadrant of a circle, with the convex margin situated caudally, lining the anterior margin of the gill chamber.

Size can be back-calculated with equations 29 to 32 and measurements taken on the subopercle as indicated on figure 11C.

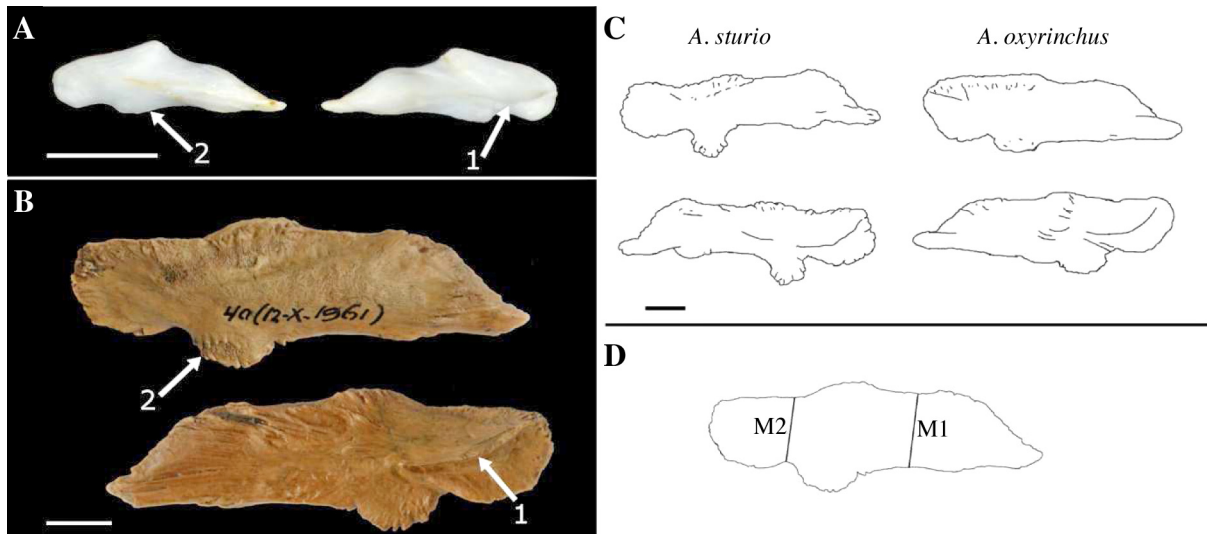Equation 29: TL = 4.6561 M1$^{0.8701}$ (R^2 = 0.96, n = 53)

Figure 17. - Dentary. **A**: Ventral and dorsal view of the left dentary from *A. oxyrinchus* (RBINS 24792); **B**: Left archaeological dentary of *A. oxyrinchus*, ventral and dorsal view; **C**: Ventral and dorsal view of the left dentary from *A. sturio* and *A. oxyrinchus*, redrawn from Desse-Berset (2011b); **D**: Measurements on the dentary as defined by Desse-Berset (1994, 2011b). Arrow 1: medial ridge; Arrow 2: processus. Scale bars = 1 cm.
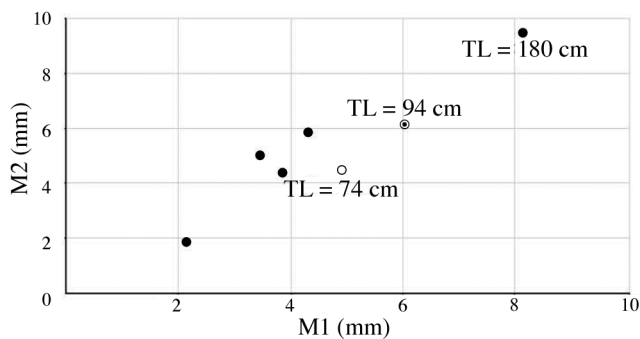

Figure 18. - Relationship between measurements M1 and M2 on the dentary from modern sturgeons of known length (adapted from Desse-Berset, 1994). ● Data of modern *A. sturio* from Desse-Berset, 1994; ○ RBINS 24792, *A. oxyrinchus*; ◉ BAI 1884, morphologically identified *A. sturio*.
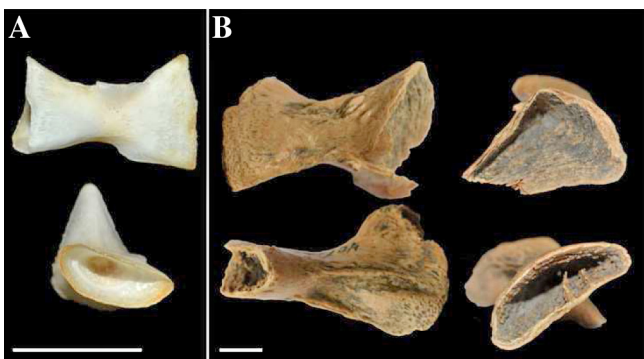

Figure 19. - Hyomandibula. **A**: Hyomandibula from *A. oxyrinchus* (RBINS 24792), lateral view and perpendicular view of the proximal end; **B**: Archaeological hyomandibula, lateral view and perpendicular view of the distal and proximal end (latter two not to scale). Note the shape differences between the distal, triangular end and the proximal, oval, squatted ends of the bone. Scale bars = 1 cm.

Equation 30: $TL = 2.8525\ M2^{0.8907}$ ($R^2 = 0.97, n = 52$)
Equation 31: $TL = 4.6870\ M3^{0.8290}$ ($R^2 = 0.93, n = 50$)
Equation 32: $TL = 3.2789\ M1^{0.3631}\ M2^{0.5352}$ ($R^2 = 0.98$, $n = 52$)

Branchiostegals

The branchiostegals are part of the opercular series and are found ventrally to the subopercle. Although there can be more than one branchiostegal present on the left or right side of the animal (Hilton *et al.*, 2011), only one of them is easily recognisable (Fig. 12). This bone has a distinctive shape with a large unornamented area, and only a small, slightly protruding ornamented area.

Palatoquadrate and associated bones, and lower jaw
Palatopterygoid

The palatopterygoid is the largest bone of the palatoquadrate and is characterised by one sharp medial and one sharp lateral processus, a bony ridge on the dorsal side and two foramina on the ventral side (Fig. 13A, B, C).

Based on the depictions of the palatopterygoids in Desse-Berset (2011b: fig. 3.5) it appears that the medial processus is more strongly developed than the lateral processus in *A. sturio* (Fig. 13C), while in *A. oxyrinchus*, the medial processus is narrower than the lateral one, although it is not clear to us if these are the species-specific differences mentioned in the text (Desse-Berset, 2011b). It is obvious, as also mentioned by Desse-Berset (2011b) that the shape is generally rather similar between both species, which probably explains why we found it hard to apply the described criteria to the archaeological palatopterygoids we investigated (e.g. Fig. 13B).

Desse-Berset (1994) indicates two measurements on the palatopterygoid (Fig. 13D), that she plotted for modern *A. sturio* (Fig. 14) of known length and age. The same measurements taken on our *A. oxyrinchus* specimen (RBINS 24792, M1 = 3.1 mm, M2 = 5.7 mm) and on a morphologically identified *A. sturio* specimen (BAI 1884, M1 = 7.1 mm, M2 = 9.5 mm) have been added to the graph. This graph allows making rough estimates of sturgeon lengths, based on isolated palatopterygoids.

Dermopalatine

The dermopalatine is a non-ornamented, curved bone from the mouth roof of the sturgeon (Fig. 15). The lateral part of the bone is thinner than the medial part, which is characterized by a concave depression (fossa). The specific shape differences of the dermopalatine that have been described for *A. sturio* and *A. oxyrinchus* by Desse-Berset (2011b) are easier to apply than those of the palatopterygoid. The medial part of the *A. sturio* dermopalatine is spade-shaped, protruding and corresponds to one third of the total length of the bone. In *A. oxyrinchus*, the medial part of the dermopalatine is less developed and corresponds to less than half of the bone, which can be observed on the modern specimen in figure 15A. Figure 15B depicts an archaeological dermopalatine with the typical *A. oxyrinchus* morphology, and figure 15C shows the typical *A. sturio* morphology.

Desse-Berset (1994) indicates two measurements on the dermopalatine (Fig. 15D), that she plotted for modern *A. sturio* (Fig. 16) of known length and age. The same measurements taken on our *A. oxyrinchus* specimen (RBINS 24792, M1 = 4.6 mm, M2 = 2.1 mm) and on a morphologically identified *A. sturio* specimen (BAI 1884, M1 = 7.8 mm, M2 = 2.5 mm) have been added to the graph. This graph allows making rough estimates of sturgeon lengths, based on isolated dermopalatines.

Dentary

The dentary is the largest bone of the lower jaw. The bone is rectangular but tapered, with a charac-

teristic ridge on the medial side and a processus (Fig. 17). The differences in shape between the dentaries of *A. sturio*

Figure 20. - Isolated elements of the branchial arches or the hyoid (with the exclusion of the hyomandibula). **A**: Modern *A. oxyrinchus* (RBINS 24792); **B**: Archaeological remains of the hyoid or branchial arches. Scale bars = 1 cm.
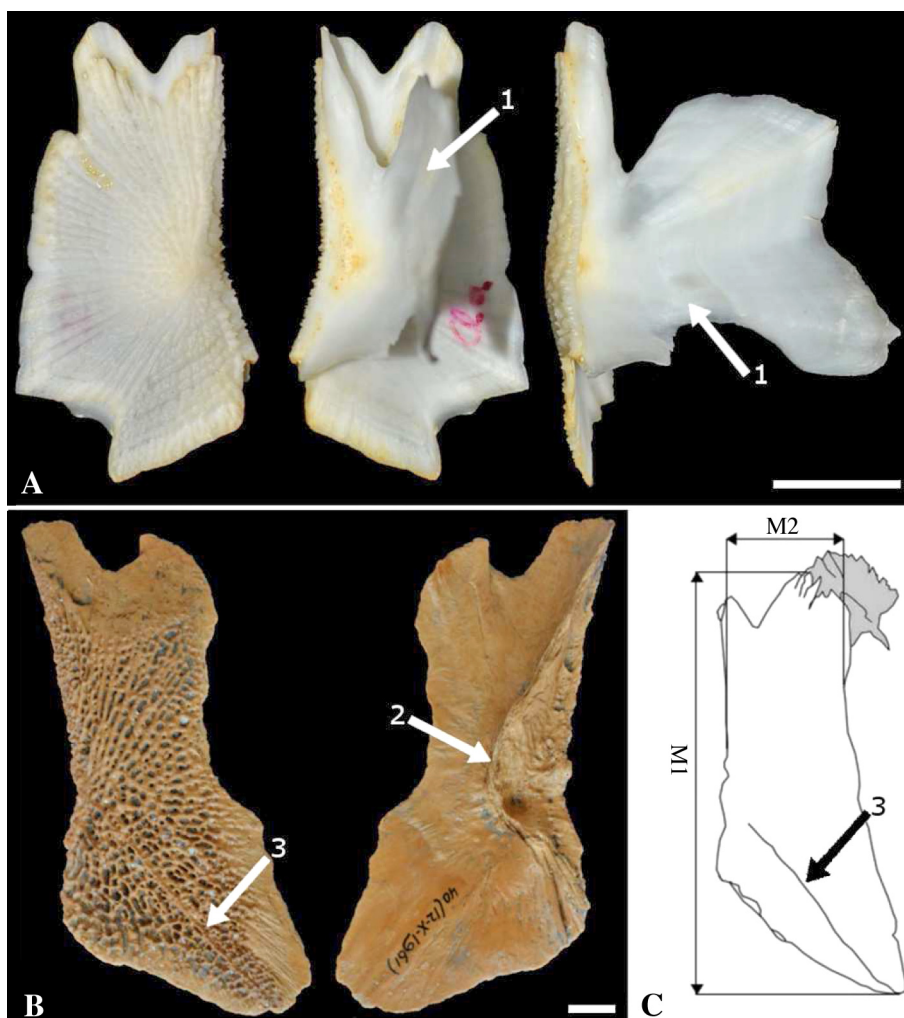

Figure 21. - Clavicle. **A**: Left clavicle (ventral, dorsal and lateral view) from *A. oxyrinchus* (RBINS 24792); **B**: Archaeological right clavicle, ventral and dorsal view; **C**: Possible measurements on the clavicle for size reconstruction. Arrow 1: dorsal membrane bone lamina; arrow 2: distinctive curve formed by broken lamina; arrow 3: straight line in the surface pattern. Scale bars = 1 cm.
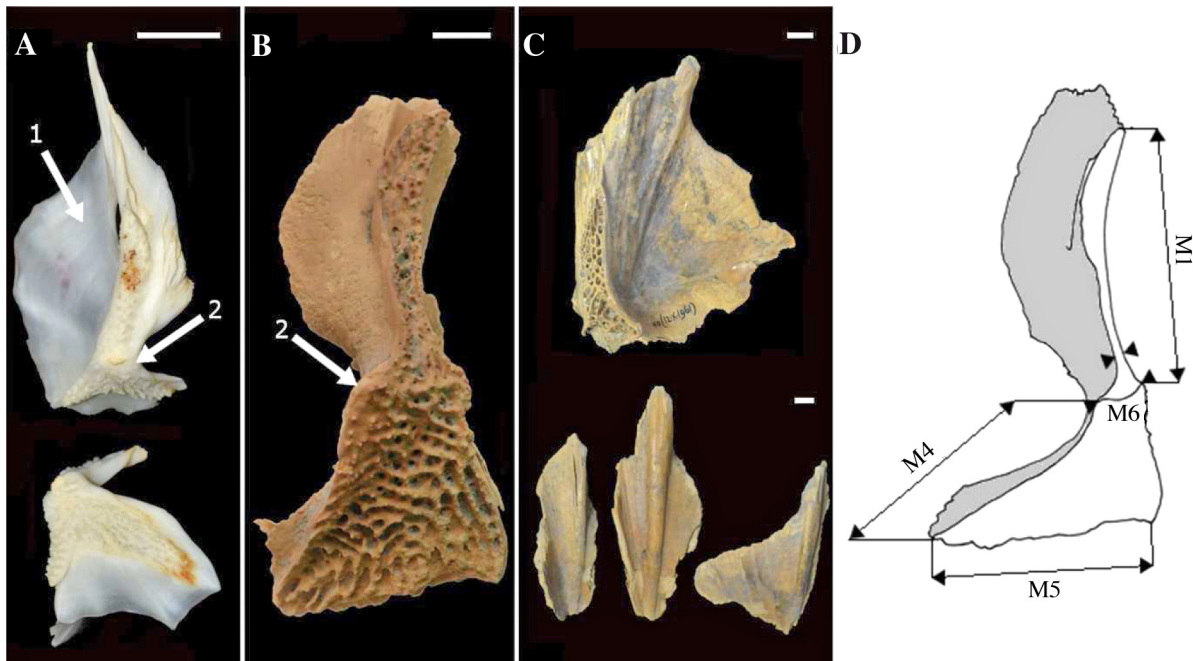
Figure 22. - Cleithrum. **A**: Lateral and ventral view of the left cleithrum from *A. oxyrinchus* (RBINS 24792); **B**: Archaeological right cleithrum, latero-ventral view; **C**: Part of an archaeological right cleithrum, lateral view, and typical lamina fragments of broken cleithra, rostral view; **D**: Possible measurements on the cleithrum for size reconstruction. Arrow 1: medial membrane bone lamina; arrow 2: incision between the dorso-lateral processus and the ventral surface. Scale bars = 1 cm.
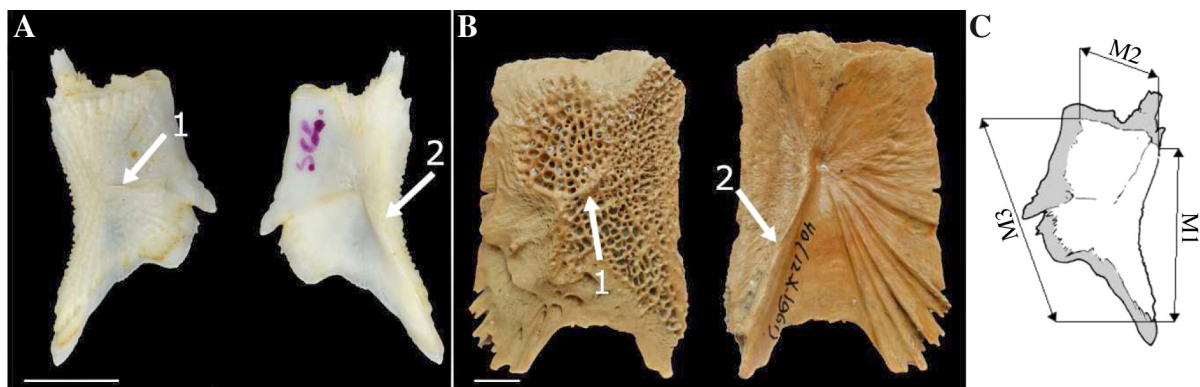

Figure 23. - Supracleithrum. **A**: Lateral and medial view of the left supracleithrum from *A. oxyrinchus* (RBINS 24792); **B**: Lateral and medial view of right supracleithrum from an archaeological specimen; **C**: Possible measurements on the supracleithrum for size reconstruction. Arrow 1: crest near the centre of the bone; Arrow 2: thickened backbone. Scale bars = 1 cm.

and *A. oxyrinchus* that have been described by Desse-Berset (2011b) allow a species identification when the archaeological bone is sufficiently well preserved. The processus of the dentary is more strongly developed in *A. sturio* than in *A. oxyrinchus*. The articular side is slightly inferior to half of the total length of the bone in *A. sturio*, while in *A. oxyrinchus* it is slightly superior (Fig. 17C). The dentary of *A. oxyrinchus* is stockier and less sinuous compared to that of *A. sturio*.

Desse-Berset (1994) indicates two measurements on the dentary (Fig. 17D), that she plotted for modern *A. sturio* (Fig. 18) of known length or age. The same measure-ments taken on our *A. oxyrinchus* specimen (RBINS 24792, M1 = 4.9 mm, M2 = 4.4 mm) and on a morphologically identified *A. sturio* specimen (BAI 1884, M1 = 6.0 mm, M2 = 6.1 mm) have been added to the graph. In a more recent publication, Desse-Berset (2011b) provided regression equations for size reconstruction for *A. sturio* (TL = 192.14 M1 + 44.723, R^2 = 0.96) and *A. oxyrinchus* (TL = 124.04 M1 + 356.37, R^2 = 0.91), based on 8 and 11 reference specimens respectively. Applying the *A. oxyrinchus* equation on M1 of the dentary from our *A. oxyrinchus* specimen (RBINS 24792) gave a back-calculated length of 96.4 cm, which is an error of 30% compared to the actual total length of 74 cm.

This relatively large error can possibly be explained by the extrapolation of the model, which was developed on specimens that were all more than 1 metre in length.

Hyoid and gill arches

The hyomandibula is the only element of the hyoid arch that can be recognised easily (Fig. 19). The other elements (interhyal, anterior and posterior ceratohyal and hypohyal) are more or less similar in shape to isolated elements of the branchial arches (Fig. 20). All of these elements are tubular, but the hyomandibula can be distinguished by its proximal squatted end and its triangular-shaped distal end. Moreover, it has typical concentric circles on the inside. In the gill arch elements and the hyoid bones (except the hyomandibula) both ends are more or less similar in shape.

Figure 24. - Pectoral fin spine. **A**: Lateral, dorsal, ventral and medial view of the left pectoral fin spine of *A. oxyrinchus* (RBINS 24792); **B**: Lateral, dorsal, ventral and medial view of an archaeological right pectoral fin spine; **C**: Possible measurements on the pectoral fin spine for size reconstruction. Arrow 1: striations; arrow 2: knuckle. Scale bars = 1 cm.

Bones of the pectoral girdle

Clavicle

The clavicle is a quadrilateral bone with a large dorsal membrane bone lamina (Fig. 21A), which is part of the opercular wall (Findeis, 1997). This lamina is often broken in archaeological bones and its remnants form a distinctive curve at the dorsal median edge of the bone (Fig. 21B). The ventral, ornamented side of the bone often displays a characteristic straight line in the surface pattern from the centre of the bone to the medio-caudal point of the clavicle (Figs 21C).

Size can be back-calculated with equation 33 to 35 with measurements on the clavicle as indicated on figure 21C.
Equation 33: TL = 1.6656 M1$^{0.9978}$ (R^2 = 0.97, n = 38)
Equation 34: TL = 5.6473 M2$^{0.9254}$ (R^2 = 0.92, n = 39)
Equation 35: TL = 2.1388 M1$^{0.7371}$ M2$^{0.2649}$ (R^2 = 0.98, n = 38)

Cleithrum

The cleithrum has a small, ornamented dorso-lateral processus, which is continuous with the larger ornamented ventral surface of the bone (Fig. 22). As shown in figure 22A and B, there is a distinctive incision between the dorsolateral processus and the ventral surface. The cleithrum is also characterised by a large medial membrane bone lamina (Fig. 22A), which forms the opercular wall together with the lamina of the clavicle (Findeis, 1997). In archaeological
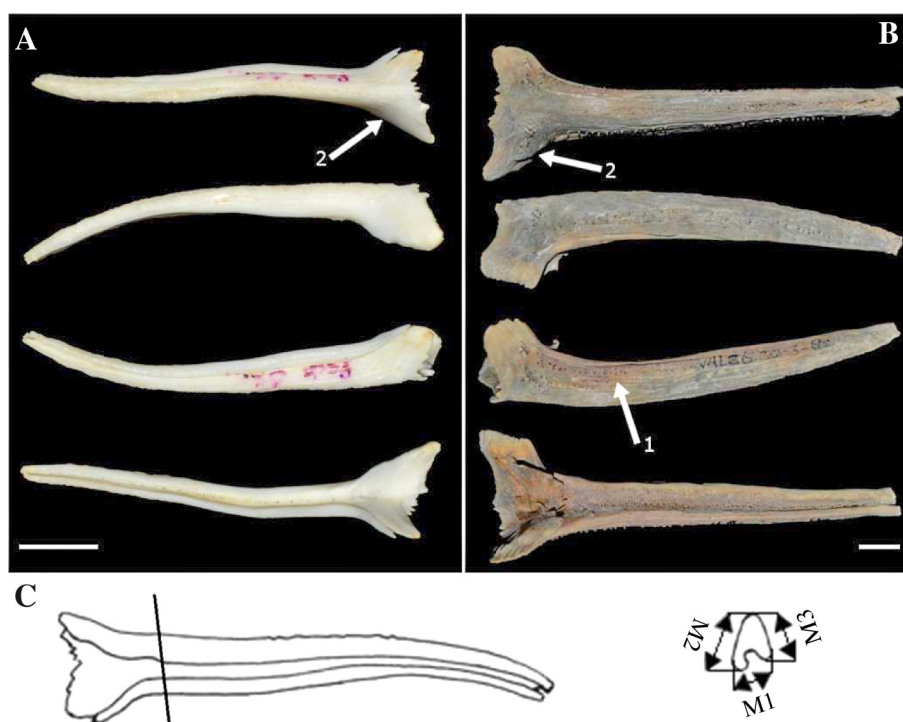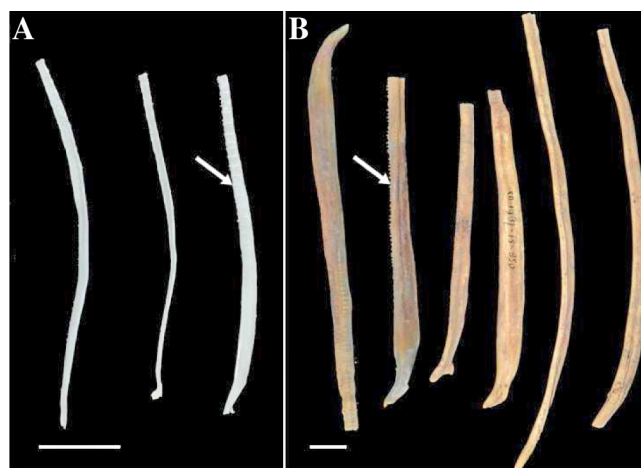

Figure 25. - Fin rays. **A**: Rays from *A. oxyrinchus* (RBINS 24792); **B**: Archaeological rays. Arrows: tubercles on edges. Scale bars = 1 cm.

remains, these lamina are often missing (e.g. Fig. 22B) but can be found in fragmented state (Fig. 22C).

Size can be back-calculated with equations 36 to 40 and measurements taken on the cleithrum as shown in figure 22D.
Equation 36: TL = 3.9167 M1$^{0.9477}$ (R^2 = 0.92, n = 44)
Equation 37: TL = 6.7438 M4$^{0.8879}$ (R^2 = 0.82, n = 37)

Table I. - Equations and R^2 values for the reconstruction of TL (cm) based on measurements on dorsal, lateral and ventral scutes (mm) (from Thieren and Van Neer, in press). The minimum value for each measurement (Min) to attain a back-calculated length of > 1m TL is also given for the lateral and dorsal scutes. Measurements are indicated on Fig. 27E for lateral scutes, Fig. 28C for dorsal scutes and Fig. 29E for ventral scutes.

|	Lateral			Dorsal			Ventral	
	All scutes			All scutes			Excluding last scute	
	Equation	R^2	Min (mm)	Equation	R^2	Min (mm)	Equation	R^2
M1	$7.816 + 2.10\,M1_{max}$	0.91	43.9	$1.937 + 2.45\,M1_{max}$	0.91	40.0	$-8.939 + 4.21\,M1_{MaxExclVlast}$	0.82
M2	$0.935 + 4.78\,M2_{max}$	0.89	20.7	$10.324 + 1.97\,M2_{max}$	0.90	45.5	$-1.797 + 3.74\,M2_{MaxExclVlast}$	0.86
M3	$7.865 + 8.51\,M3_{max}$	0.87	10.8	$10.006 + 3.89\,M3_{max}$	0.90	23.1	$19.252 + 5.77\,M3_{MaxExclVlast}$	0.81
M4	$5.182 + 3.47\,M4_{max}$	0.88	27.3	$-5.935 + 3.95\,M4_{max}$	0.81	26.8	$11.906 + 5.74\,M4_{MaxExclVlast}$	0.62
M5	$14.847 + 3.70\,M5_{max}$	0.83	23.0	$11.756 + 2.64\,M5_{max}$	0.81	33.4	$14.316 + 4.73\,M5_{MaxExclVlast}$	0.75
M6	$6.181 + 2.82\,M6_{max}$	0.91	33.3	$5.759 + 2.99\,M6_{max}$	0.88	31.5	$-12.104 + 4.86\,M6_{MaxExclVlast}$	0.83
M7	$8.459 + 4.08\,M7_{max}$	0.87	22.4	$-2.421 + 3.89\,M7_{max}$	0.77	26.3	$-35.184 + 8.06\,M7_{MaxExclVlast}$	0.74
M8	$6.404 + 4.00\,M8_{max}$	0.90	23.4	$3.688 + 2.84\,M8_{max}$	0.84	33.9	$-10.607 + 5.76\,M8_{MaxExclVlast}$	0.78
M9	$14.325 + 3.66\,M9_{max}$	0.86	23.4	$0.949 + 3.11\,M9_{max}$	0.88	31.8	$-4.427 + 4.77\,M9_{MaxExclVlast}$	0.81
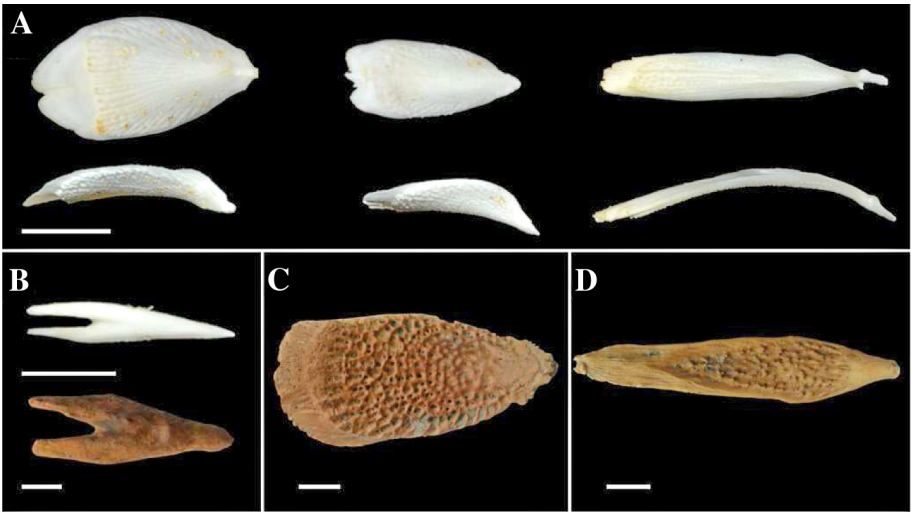
Figure 26. - Fulcra. **A**: Dorsal, anal and dorsal caudal fin basal fulcrum from *A. oxyrinchus* (RBINS 24792), dorsal and side view; **B**: Forked caudal fulcrum from *A. oxyrinchus* (RBINS24792) and an archaeological one, dorsal view; **C**: Archaeological dorsal or anal fin basal fulcra; **D**: Archaeological dorsal or ventral caudal fin basal fulcrum. Scale bars = 1 cm.

Equation 38: TL = $5.6652\,M5^{0.9178}$ ($R^2 = 0.91$, n = 37)

Equation 39: TL = $11.4734\,M6^{0.9453}$ ($R^2 = 0.88$, n = 36)

Equation 40: TL = $4.3833\,M1^{0.7136}\,M6^{0.3072}$ ($R^2 = 0.96$, n = 34)

Supracleithrum

The supracleitrum has a slightly concave anterior margin bordering the gill chamber and a large ornamented lateral surface (Fig. 23). This surface has a distinctive small, low crest or ridge near the centre of the bone. The ornamented surface has a more or less triangular shape and extends up to the concave anterior margin, which can make it rough to the touch. On the backside of the bone, a thickened 'backbone'

runs from the centre to the anteroventral tip of the bone (Fig. 23A, B).

Size can be back-calculated with equations 41 to 43 with measurements taken on the supracleithrum as shown in figure 23C.

Equation 41: TL = $2.4373\,M1^{0.9917}$ ($R^2 = 0.96$, n = 49)

Equation 42: TL = $4.0351\,M2^{1.0147}$ ($R^2 = 0.93$, n = 49)

Equation 43: TL = $2.9901\,M3^{0.9345}$ ($R^2 = 0.96$, n = 38)

Fins and fin supports

Pectoral Fin Spine

The pectoral fin spine typically displays longitudinal ridges or striations and has a distinctive 'knuckle' near the articulation, which can be used to decide laterality (Fig. 24A, B), as the dorsal side of the knuckle is longer than the ventral side.

Size can be back-calculated with equations 44 to 46 and measurements taken on the pectoral fin spine as indicated on figure 24C. Measurements are taken right behind the knuckle at the proximal end of the spine.

Equation 44: TL = $16.6327\,M1^{1.0134}$ ($R^2 = 0.95$, n = 28)

Equation 45: TL = $13.9741\,M2$ ($R^2 = 0.94$, n = 40)

Equation 46: TL = $13.8491\,M3^{0.9845}$ ($R^2 = 0.86$, n = 29)

Fin ray

The fin rays are easily recognisable by their long, flattened structure and often display small tubercles on their
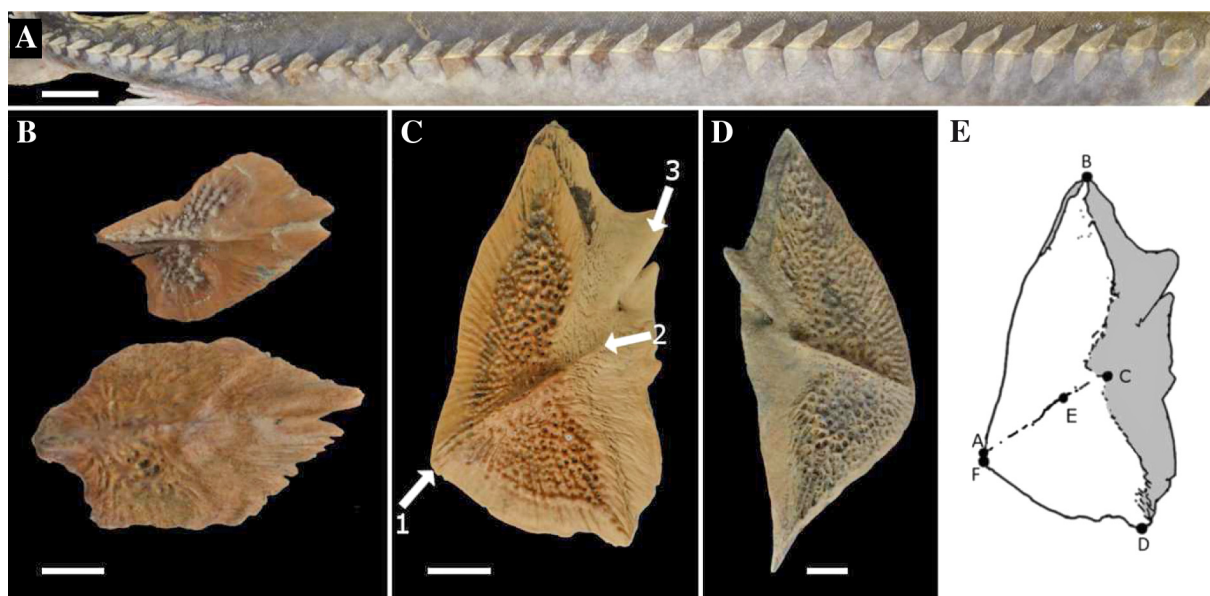
Figure 27. - Lateral scutes. **A**: Complete right lateral row from a modern *A. sturio* (NHM 2015.2.18.1, 160.5 cm TL); **B**: Archaeological right lateral scutes from the back of the row; **C**, **D**: Right and left lateral scute from the front or middle of the row; **E**: Right lateral scute with the possible measurements for size reconstruction: M1: B-D; M2: F-C; M3: A-E; M4: B-E; M5: B-C; M6: B-F (caudal edge of the dorsal part); M7: D-E; M8: D-C; M9: D-F (caudal edge of the ventral part). Arrow 1: caudal point; arrow 2: frontal edge of the ridge; Arrow 3: dorsally pointed thickened fold. Scale bars: A = 10 cm; B, C, D = 1 cm.
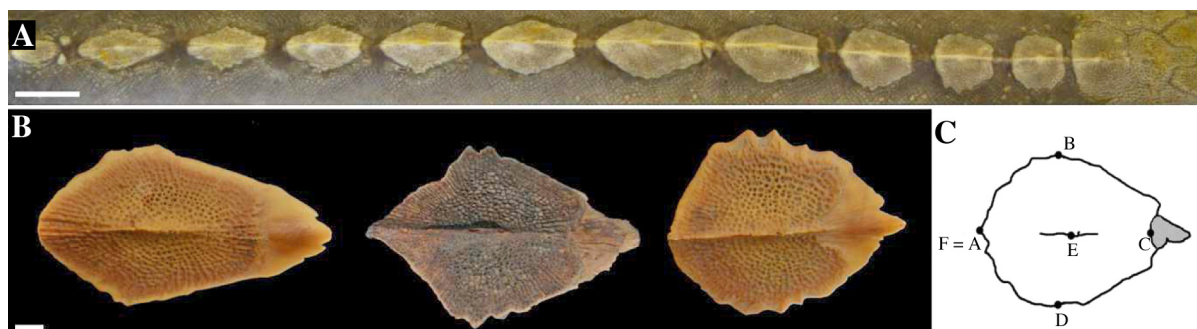

Figure 28. - Dorsal scutes. **A**: Complete dorsal scute row and dorsal fin fulcrum from a modern *A. sturio* (NHM 2015.2.18.1, 160.5 cm); **B**: Archaeological dorsal scutes; **C**: Possible measurements on the dorsal scutes for size reconstruction: M1: B-D; M2: F = A-C; M3: A = F-E; M4: B-E; M5: B-C; M6: B-F = A; M7: D-E; M8: D-C; M9: D-F = A. Scale bars: A = 10 cm; B = 1 cm.

edges (Fig. 25). These elements are not suitable for reliable size reconstructions.

Fulcra

The scute-like basal fulcra have an obovate to shoehorn-like shape and are associated with the dorsal, anal and caudal fin. The dorsal and anal fin basal fulcra (Fig. 26A, C) are similar and wider compared to the longer and thinner ventral and dorsal caudal fin basal fulcra (Fig. 26A, D). Following the dorsal caudal fin basal fulcra, a series of forked fulcra lines the dorsal edge of the caudal fin (Fig. 26B). These elements were not considered for size reconstructions. Crude size estimations can be made through direct comparison with specimens of known length.

Scutes

Sturgeons are characterized by five rows of scutes alongside the body: one dorsal, two lateral and two ventral rows (Fig. 1A). Albeit that scutes from the different rows are easily recognisable by their shape (see Figs 27-29), scute shape is similar in *A. oxyrinchus* and *A. sturio* and therefore does not allow species identification (Desse-Berset, 2011b; Thieren and Van Neer, in press).

Back-calculation of sturgeon lengths with scutes is not accurate because of the large size variation within one row, combined with the difficulties to exactly determining the original position of an isolated, archaeological scute. Earlier attempts to establish fish length from lateral scutes have been published, for example, for *A. sturio* by Brinkhuizen (1989: 254-255) who took into account the variation along one row
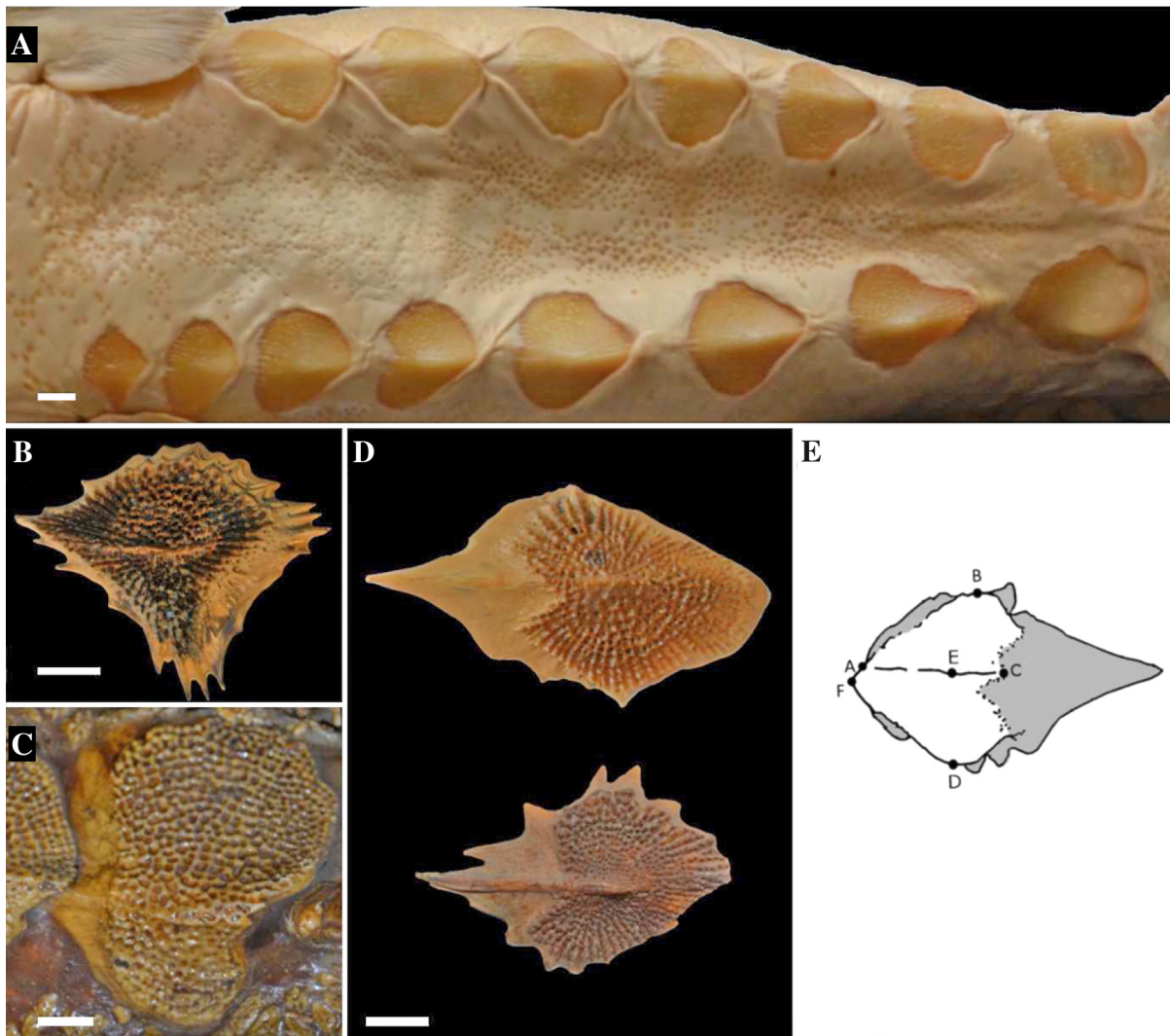
Figure 29. - Ventral scutes. **A**: Complete ventral scute rows from a modern *A. oxyrinchus* (NRM 60821, 99 cm TL); **B**: Archaeological first right ventral scute; **C**: Last right ventral scute from a modern *A. oxyrinchus* (MNHN-IC-0000-3113, 158 cm TL); **D**: Archaeological left and right ventral scute; **E**: Possible measurements on the ventral scutes for size reconstruction: M1: B-D; M2: F-C; M3: A-E; M4: B-E; M5: B-C; M6: B-F (caudal edge of the lateral part); M7: D-E; M8: D-C; M9: D-F (caudal edge of the ventral part). Scale bars = 1 cm.

by providing a minimum and maximum TL estimation for each measurable archaeological scute. Desse-Berset (2011b) provided a regression equation for the calculation of the total length of *A. oxyrinchus* on the basis of the mean width of the dorsal scutes (excluding the first dorsal scute and the dorsal fin basal fulcrum) and stipulates also that the reconstructed size would be more accurate if it would have been possible to establish the exact provenance of the scutes within the row. Thieren and Van Neer (in press), provided equations for size reconstruction (Tab. I) based on different scute measurements of lateral (Fig. 27E), dorsal (Fig. 28C) and ventral scutes (Fig. 29E). These equations were tested on scute measurements from different museum specimens, which showed that only rough estimations of length are possible. When the back-calculated length exceeded 1 m, the actual

length was indeed larger than 1 m, even though the back-calculated length itself was not accurate. Back-calculated lengths under 1 m occurred with measurements on scutes of specimens both larger and smaller than 1 m TL. So, although these models do not allow precise size reconstruction, it can be ascertained if a specimen was larger than 1 m TL. When the back-calculations indicate a fish larger than 1 m, it is safe to assume that the total length of the sturgeon indeed exceeds 1 m TL. For scutes with back-calculated lengths below 1 m, no reliable conclusions can be drawn concerning the original size of the sturgeon. Table I also includes the minimum values needed for each measurement to attain back-calculated lengths larger than 1 m TL for the lateral and dorsal scutes. Scutes with measurements equal to or larger than this minimum value can be identified to species on the basis of their

Figure 30. - Scutes behind the dorsal fin of *A. oxyrinchus* (NRM 35438; 154 cm TL). Scale bar = 1 cm.

ornamentation pattern. Size reconstruction based on ventral scutes should ideally be done through direct comparison with specimens of known length since the back-calculation of length is not that accurate.

Lateral scutes

The lateral scutes are found on the level of the lateral line on the right and left side of the body. The row starts directly behind the supracleithrum and ends in the caudal fin with the last scute having a ridge or crest alongside its short axis. The shape of the ornamented part of the scute is more scalene triangular-like, with the obtuse angle pointing caudally (Fig. 27C). The articulation area of the scute is smooth and lies beneath the previous scute in small animals. If that area is also considered, the scutes are more rhomboidal shaped. The shape of the scutes changes from the beginning to the end of the row (Fig. 27A), with the ornamented part of scutes in the beginning of the row being more triangular-like (Fig. 27C, D). The ornamented part of the scutes in the back of the row is more dorso-ventrally compressed and antero-posteriorly elongated (Fig. 27B).

Right-sided scutes can be distinguished from scutes from the left side of the body by different characteristics (Fig. 27C). First of all, the dorsal half (the part above the crest or ridge) of the scute is larger and more elongated than the ventral half below the ridge. The caudal edge of the dorsal part is rather straight, while that of the ventral half is curved (Fig. 27E). Secondly, the ridge on the lateral scutes ends in the caudal point of the scute, but not always. If not, the caudal point of the scute is situated in the ventral half of the scute, below the ridge (Fig. 27C). Thirdly, the frontal end of the ridge, in the unornamented articulation area of the scute, bends slightly dorsally (Fig. 27C). Lastly, there is a thickened fold pointing dorsally in the unornamented articulation area (Fig. 27C). Deciding laterality can be difficult for scutes from the back of the row.

Dorsal scutes

Dorsal scutes are the largest of the three-scute types. They are symmetrical and more or less rhomboid, with the
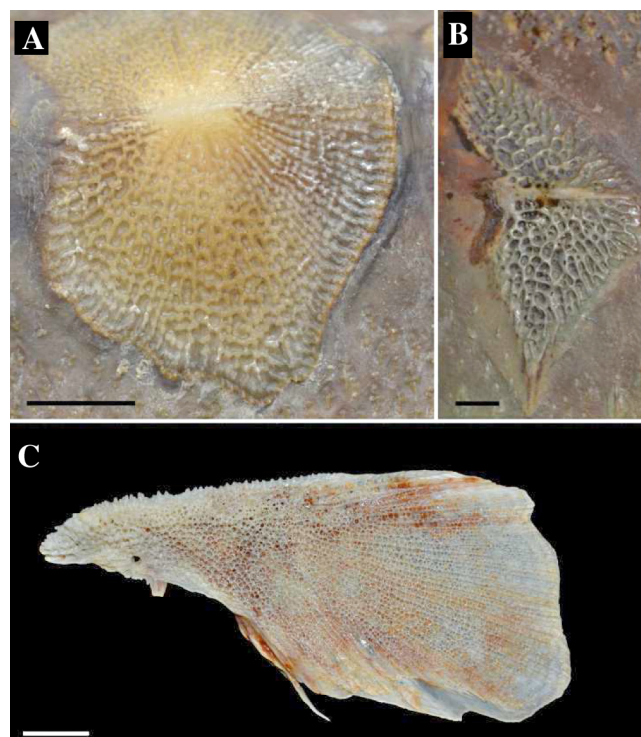

Figure 31. - Alveolar ornamentation type. **A**: Alveolar pattern with tubercular characteristics at the edge in *A. oxyrinchus* (NRM 60821, 4th dorsal scute, 99 cm TL); **B**: Alveolar pattern in a large *A. oxyrinchus* (MHNNZ 19558, 6th left lateral scute, 276 cm TL); **C**: Lacrimale-suborbitale from *Trigla lucerna* (RBINS 23663; 47.5 cm SL). Note the alveolar-like ornamentation. Scale bars = 1 cm.

ornamented part shaped as a regular pentagon, although there is quite some inter- and intra-individual variation (Fig. 28). In general, dorsal scutes become more elongated towards the end of the row.

Ventral scutes

The ventral scutes are paired and asymmetrically shaped (Fig. 29). They are situated in the extension of the medio-caudal point of the clavicles between the pectoral and pelvic fins. In general, these scutes have an ornamented area
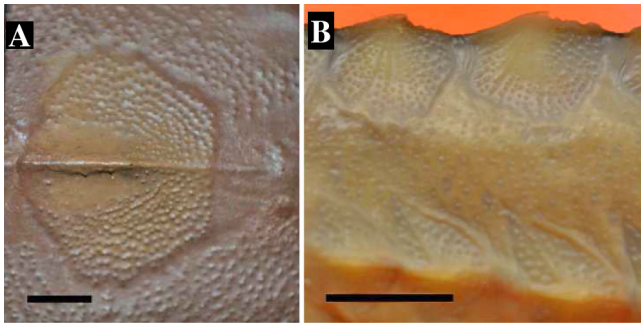
Figure 32. - Examples of tubercular ornamentation types in *A. sturio*. **A**: 4th dorsal scute (overpainted) from a specimen of 153 cm TL (MNHN-IC-0000-3119); **B**: 2nd and 3rd dorsal and 1st to 3rd left lateral scute from a specimen of 38 cm TL (NRM 21708). Scale bars = 1 cm.

with a more asymmetrical, spade-like shape, with the ornamented point directed caudally. The lateral part of the scute is smaller than the ventral part. The lateral part also has a straighter caudal edge than the ventral part (Fig. 29E). The first (Fig. 29B) scute has an irregular shape while the last (Fig. 29C) scute is more rounded. This scute has a larger rounded ventral part and a smaller rounded lateral part.

Accessory scutes

In addition to the five regular scute rows, *A. oxyrinchus* and *A. sturio* also have scutes behind the dorsal and ventral fins and behind and on the left and right side of the anal fin (Vecsei *et al.*, 2001) (e.g. Fig. 30). These scutes are flat, have an irregular shape and lack the crest observed on the regular scutes.

Species identification based on ornamentation types

With the exception of the aforementioned shape differences of the palatopterygoid, dermopalatine and dentary described by Desse-Berset (2011b), archaeological sturgeon bones (*A.sturio*/*A. oxyrinchus*) can only be morphologically identified to species by the surface pattern of the dermal bones. Although the ornamentation pattern of *A. oxyrinchus* is described as alveolar and that of *A. sturio* as tubercular (Magnin, 1964), we have found considerable variation within each species, and sometimes even within the same individual or within a single bone of an individual (Thieren *et al.*, unpubl. data). It appears that a size-related intraspecific difference occurs in dermal bone surface ornamentation. Disregarding the size of the animal, bones with an alveolar ornamentation type (Fig. 31A, B) can indeed be assigned to *A. oxyrinchus*, which is in most cases correct as shown by genetic validation. The alveolar surface pattern is very typical for *A. oxyrinchus*, but should not be mistaken with that of gurnards (*Trigla* sp.), who also display an alveolar-like pattern on the surface of their bones (Fig. 31C). However, the alveoli in gurnards are finer, with very thin septa, and underneath the ornamentation some small holes can be seen under a binocular, which are absent in sturgeon. Finally, the bones of *Trigla* sp. are in most cases lighter and thinner than those of sturgeon and they tend to have a glossy appearance.

For the bones with the tubercular ornamentation type (Fig. 32), species identification is not as straightforward, as this type is also observed in small (< 1 m TL) *A. oxyrinchus* and in lateral scutes from the back of the lateral scute rows in *A. oxyrinchus* specimens that display an alveolar pattern in their other dermal bones. In some dermal bones, it was also observed that the alveolar ornamentation pattern became more tubercular-like towards the edges of the bone (e.g. Fig. 31A). Therefore, bones with a tubercular ornamentation type should only be assigned to *A. sturio* if they are not from the back of the lateral row (See Lateral scutes section) and if their back-calculated length is larger than 1m. Care should also be taken not to identify marginal bone fragments with tubercular ornamentation.

CONCLUSION

This paper is intended as a practical guide to the identification of sturgeon remains (*A. oxyrinchus*/*A. sturio*) from European archaeological sites in the Atlantic, North Sea and Baltic Sea region. The descriptions above show that the shape of most isolated skeletal elements is similar in *A. sturio* and *A. oxyrinchus*, with the exception of the palatopterygoid and, in particular, the dentary and dermopalatine that have species-specific features. After the identification of an archaeological sturgeon bone to its skeletal element, length reconstruction of the corresponding fish can be carried out with the aid of regression equations that we provide and that are valid for both species. Species identification for elements other than the dentary, dermopalatine and palatopterygoid, is based on the ornamentation of the external surface of the dermal bones and can be carried out with rather great confidence on remains from sturgeons that were one metre or more in length.

gium) for providing an *Acipenser oxyrinchus* specimen that has been prepared as a skeleton, now registered in the collections of the Royal Belgian Institute of Natural Sciences (RBINS 24792).

We also thank the following authorities that made the archaeological sturgeon remains available for analysis: the Museum of London (UK), the Agentschap Onroerend Erfgoed (Flanders, Belgium) and in The Netherlands: Groningen Institute of Archaeology; Museum Het Valkhof (Nijmegen); Afdeling Archeologie (Gemeente Den Haag); Archeologisch depot (Provincie Utrecht); Rijksmuseum van Oudheden (Leiden); Bureau Monumentenzorg en Archeologie (Gemeente Rijswijk); Provinciaal Archeologisch Depot Zuid-Holland; Bureau Oudheidkundig Onderzoek (Rotterdam).

REFERENCES

ARCHAEOLOGICAL FISH RESOURCE, 2011. - Archaeological Fish Resource. <http://fishbone.nottingham.ac.uk/>. Dept of Archaeology, Univ. of Nottingham. Accessed on 18 Feb. 2015.

BENECKE N., 1986 - Some remarks on sturgeon fishing in the southern Baltic region in medieval times. *In*: Fish and Archaeology. Studies in Osteometry, Taphonomy, Seasonality and Fishing Methods (Brinkhuizen D.C. & Clason A.T., eds.), pp. 9-17. B.A.R. International Series 294. Oxford: B.A.R.

BRINKHUIZEN D.C., 1989. - Ichthyo-archeologisch onderzoek: Methoden en toepassing aan de hand van Romeins vismateriaal uit Velsen (Nederland) [Ichtyoarchaeological research: Methods and applications based on Roman fish material from Velsen (The Netherlands]. Doctoral thesis, 312 p. Rijksuniversiteit Groningen, The Netherlands. (in Dutch)

CHASSAING O., DESSE-BERSET N., DUFFRAISSE M., HUGHES S., HÄNNI C. & BERREBI P., 2013. - Palaeogenetics of western French sturgeons spotlights the relationships between *Acipenser sturio* and *Acipenser oxyrinchus*. *J. Biogeogr.*, 40(2): 382-393.

CLASON A.T., 1967. - Animal and man in Holland's past: an investigation of the animal world surrounding man in prehistoric and early historical times in the provinces of North and South Holland. 437 p. *Palaeohistoria* XIIIA. Groningen: J.B. Wolters.

DESSE-BERSET N., 1994. - Sturgeons of the Rhône during Protohistory in Arles (6th-2nd century BC). *In*: Fish Exploitation in the Past. Proc. of the 7th meeting of the ICAZ Fish Remains Working Group (Van Neer W., ed.), pp. 81-90. *Ann. Mus. R. Afr. Cent.*, Sci. Zool., 274. Tervuren.

DESSE-BERSET N., 2009. - First archaeozoological identification of Atlantic sturgeon (*Acipenser oxyrinchus* Mitchill, 1815) in France. *C.R. Palevol.*, 8(8): 717-724.

DESSE-BERSET N., 2011a. - Ancient sturgeon populations in France through archaeozoological remains, from prehistoric time until the eighteenth century. *In*: Biology and Conservation of the European Sturgeon *Acipenser sturio* L., 1758. The Reunion of the European and Atlantic Sturgeons (Williot P., Rochard E., Desse-Berset N., Kirschbaum F. & Gessner J., eds), pp. 91-116. Berlin Heidelberg: Springer-Verlag.

DESSE-BERSET N., 2011b. - Discrimination of *Acipenser sturio*, *Acipenser oxyrinchus* and *Acipenser naccarii* by morphology of bones and osteometry. *In*: Biology and Conservation of the European Sturgeon *Acipenser sturio* L., 1758. The Reunion of the European and Atlantic Sturgeons (Williot P., Rochard E., Desse-Berset N., Kirschbaum F. & Gessner J., eds), pp. 23-52. Berlin Heidelberg: Springer-Verlag.

ERVYNCK A., VAN NEER W. & VAN DER PLAETSEN P., 1994. - Dierlijke resten. *In*: De 'Burcht' te Londerzeel. Bewoningsgeschiedenis van een motte en een bakstenen kasteel (Animal remains [The 'Castle' of Londerzeel. Occupational history of a motte and a brick castle] (Dewilde M., Ervynck A., Van Neer W., De Meulemeester J. & Van der Plaetsen P., eds), pp. 99-170. *Archeologie in Vlaanderen. Monografie* 1. Zellik: Instituut voor het Archeologisch Patrimonium. (in Dutch)

FINDEIS E.K., 1997. - Osteology and phylogenetic interrelationships of sturgeons (Acipenseridae). *Environ. Biol. Fish.*, 48(1): 73-126.

HILTON E.J., GRANDE L. & BEMIS W.E., 2011. - Skeletal anatomy of the shortnose sturgeon, *Acipenser brevirostrum* Lesueur, 1818, and the systematics of sturgeons (Acipenseriformes, Acipenseridae). *Fieldiana Life Earth Sci.*, 3: 1-168.

LUDWIG A., DEBUS L., LIECKFELDT D., WIRGIN I., BENECKE N., JENNECKENS I., WILLIOT P., WALDMAN J.R. & PITRA C., 2002. - Fish populations: when the American sea sturgeon swam east. *Nature*, 419(6906): 447-448.

LUDWIG A., ARNDT U., LIPPOLD S., BENECKE N., DEBUS L., KING T. & MATSUMURA S., 2008. - Tracing the first steps of American sturgeon pioneers in Europe. *BMC Evol. Biol.*, 8(1): 221.

LUDWIG A., MAKOWIECKI D. & BENECKE N., 2009. - Further evidence of trans-Atlantic colonization of Western Europe by American Atlantic sturgeons. *Archaeofauna*, 18: 185-192.

LYMAN R.L., 2006. - Paleozoology in the service of conservation biology. *Evol. Anthropol.*, 15(1): 11-19.

MAGNIN É., 1964. - Validité d'une distinction spécifique entre les deux acipenséridés: *Acipenser sturio* L. d'Europe et *Acipenser oxyrhynchus* d'Amérique du Nord. *Nat. Can.*, 91(1): 5-20.

MAKOWIECKI D., 2008. - Sturgeon fishing on Polish Lowland during Holocene. *In*: Archéologie du poisson. 30 ans d'archéoichtyologie au CNRS. Actes des XXVIIIe rencontres internationales d'archéologie et d'histoire d'Antibes, XIVth ICAZ Fish remains working group meeting (Béarez, P., Grouard, S. & Clavel, B., eds), pp. 327-339. Antibes: Éditions APDCA.

POPOVIĆ D., PANAGIOTOPOULOU H., BACA M., STEFANIAK K., MACKIEWICZ P., MAKOWIECKI D., KING T.L., GRUCHOTA J., WEGLENSKI P. & STANKOVIC A., 2014. - The history of sturgeon in the Baltic Sea. *J. Biogeogr.*, 41(8): 1590-1602.

THIEREN E. & VAN NEER W., 2014. - New equations for the size reconstruction of sturgeon from isolated cranial and pectoral girdle bones. *Int. J. Osteoarchaeol.* DOI: 10.1002/oa.2407

THIEREN E. & VAN NEER W., in press. - Scutes for sturgeon size reconstruction: traditional and geometric morphometric techniques applied to *Acipenser sturio* and *A. oxyrinchus*. *Archaeofauna*.

TIEDEMANN R., MOLL K., PAULUS K., SCHEER M., WILLIOT P., BARTEL R., GESSNER J. & KIRSCHBAUM F., 2007. - Atlantic sturgeons (*Acipenser sturio*, *Acipenser oxyrinchus*): American females successful in Europe. *Naturwissenschaften*, 94(3): 213-217.